PLOS ONE

Cu(II)-tyrosinase enzyme catalyst mediated synthesis of mosquito larvicidal active pyrazolidine-3,5-dione derivatives with molecular docking studies and their ichthyotoxicity analysis

Velmurugan Loganathan[1☯], SurendraKumar Radhakrishnan[1☯], Anis Ahamed[2☯], Raman Gurusamy[3☯], Omar H. Abd-Elkader[4☯], Akbar Idhayadhulla[1☯]*

1 Research Department of Chemistry, Nehru Memorial College (Affiliated Bharathidasan University), Puthanampatti, Tamilnadu, India, 2 Department of Botany and Microbiology, College of Science, King Saudi University, Riyadh, Saudi Arabia, 3 Department of Life Science, Yeungnam University, Gyeongsan, Gyeongbuk-do, South Korea, 4 Department of Physics and Astronomy, College of Science, King Saudi University, Riyadh, Saudi Arabia

☯ These authors contributed equally to this work.
* a.idhayadhulla@gmail.com

Abstract

The objective of this study was to develop pyrazolidine-3,5-dione derivatives with potential as environmentally friendly pesticides for pest control, specifically focusing on their efficacy as larvicidal agents. A novel one-pot synthesis of multicomponent pyrazolidine-3,5-dione derivatives (**1a-m**) was accomplished via the grindstone method using Cu(II)tyrosinase enzyme as a catalyst under mild reaction conditions, yielding 84%–96%. The synthesised derivatives (**1a-m**) were characterized using various spectroscopic methods (mass spectrometry, elemental analysis, FT-IR, and ^{1}H and ^{13}C NMR). NMR characterisation using DMSO-d_6 as a solvent. The larvicidal and antifeedant activities of the synthesised compounds were screened and *in silico* computational studies were performed. The larvicidal activity against *Culex quinquefasciatus* and antifeedant activity against *Oreochromis mossambicus* were evaluated. Among the synthesised compounds, compound **1c** demonstrated superior efficacy (LD$_{50}$: 9.7 µg/mL) against *C. quinquefasciatus* compared to permethrin (LD$_{50}$: 17.1 µg/mL). Regarding antifeedant activity, compounds **1a**, **1e**, **1f**, **1j**, and **1k** exhibited 100% mortality at 100 µg/mL. Molecular docking analysis was performed to assess the binding capacity of a mosquito odorant-binding protein (3OGN) from *Culex quinquefasciatus* to compound **1c**. The results revealed that compound **1c** had a docking score of -10.4 kcal/mol, surpassing that of standard permethrin (-9.5 kcal/mol). Furthermore, DFT calculations were conducted to acquire theoretical data aligned with the experimental FT-IR results. According to experimental research, compound **1c** demonstrates promising larvicidal activity against mosquito larvae of *C. quinquefasciatus*.
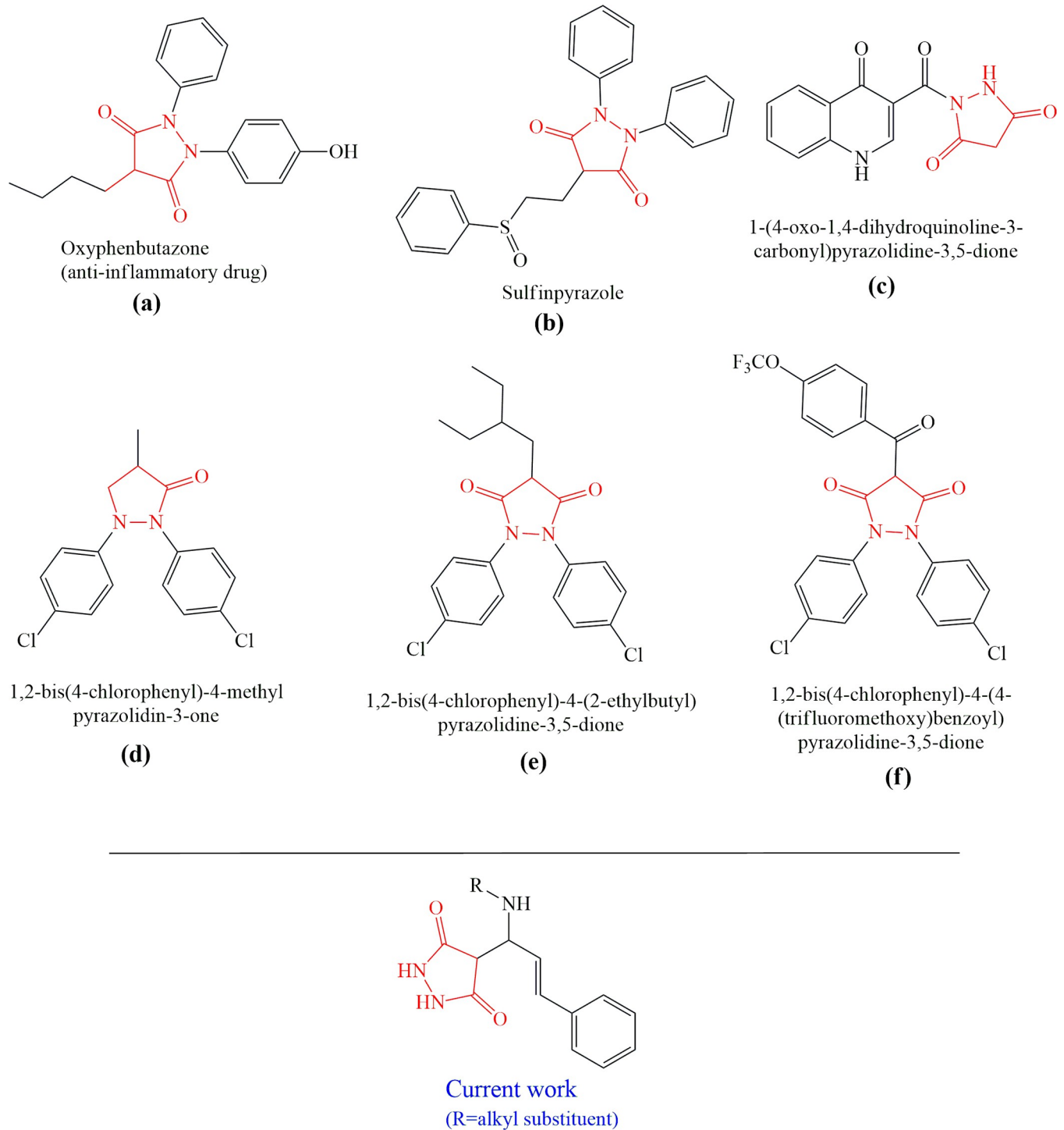
Introduction

Millions of people succumb annually to mosquito-borne illnesses like malaria, filariasis, dengue, and yellow fever, rendering mosquitoes the most perilous insects [1]. The most effective preventive measure is controlling mosquito larvae, pivotal as vectors for disease transmission. Regular application of larvicidal chemicals, notably organophosphates and insect development inhibitors, is commonly employed for this purpose [2]. However, the frequent utilization of these chemicals adversely affects unintended populations and may potentially lead to the emergence of resistant strains, raising concerns [3]. Hence, there is an imperative need for safer and more efficient approaches to control mosquito larvae.

Among these vectors, *Culex quinquefasciatus* mosquitoes are the most frequently associated with human habitats in both urban and rural areas [4, 5]. In recent years, research has been directed towards botanical pesticides as a pursuit of natural alternatives to synthetic insecticides. These alternatives are intriguing due to their versatility in roles such as growth inhibitors, insecticides, larvicides, antifeedants, repellents, or oviposition deterrents. They are natural, biodegradable, and exhibit minimal toxicity [6]. Alkaloid isoquinolines have garnered significant interest as genetic precursors to various biologically active compounds, holding promise for applications in disease treatment [7, 8] and insect management [9].

Chemists are intrigued by heterocycles and their derivatives due to the diverse biological and pharmacological attributes within this molecular family, particularly those containing nitrogen [10, 11]. The carbonyl (C = O) group in pyrazolidine-3,5-dione derivatives is pivotal for various pharmaceutical and biological activities [12]. Pyrazolidine-3,5-dione derivatives have attracted considerable attention owing to their broad spectrum of biological activities, including antitumor, anti-HIV, anti-inflammatory, COX-2 inhibitory, and significant anti-metastatic effects [13–16]. Fig 1 illustrates some bioactive pyrazolidine derivatives previously reported [11, 17, 18].

The dinuclear copper core of mushroom tyrosinase catalyses hydroxylation and oxidation processes [19–25]. $Cu(II)-O_2^{2-}$—$Cu(II)$ forms a μ-2:2 side-on bridging bond with dioxygen, where O_2^{2-} is in the oxy state. The met type [Cu(II)-Cu(II)] designates a state in which only the Cu atoms at the active site undergo oxidation and are not linked to dioxygen. Tyrosinase functions as a catalyst and contains water molecules or hydroxide ions along with Cu^{+2}, connected by one or two small ligands. Mannich-type reactions, while facilitating the formation of compounds, often encounter challenges in terms of reaction conditions, catalyst reaction time, separation, and toxicity of the final product(s) [26]. The aim of developing the Cu(II)-Tyr enzyme as a novel eco-friendly catalyst was to address the challenges of low yields, harsh conditions, and lengthy reaction times. Previously reported literature on Cu(II)tyrosinase catalysts and proteins, specifically focusing on larvicidal and antifeedant activity, was considered [27–29]. Pyrazolidine-3,5-dione derivatives have been reported to exhibit various activities. For the first time, this derivative was synthesised using Cu(II)-Tyr catalyst and screened for larvicidal and antifeedant activities.

In this study, we successfully synthesised novel one-pot multicomponent pyrazolidine-3,5-dione derivatives via the grindstone method using a Cu(II)tyrosinase catalyst. Moreover, the study aimed to investigate the larvicidal and antifeedant activities of all synthesised compounds and computationally evaluated them as potential agents against 3OGN through molecular docking simulations. Based on the findings of this study, the synthesised derivatives demonstrate larvicidal activity and potential as eco-friendly pesticides for pest control.

Oxyphenbutazone
(anti-inflammatory drug)

(a)

Sulfinpyrazole

(b)

1-(4-oxo-1,4-dihydroquinoline-3-carbonyl)pyrazolidine-3,5-dione

(c)

1,2-bis(4-chlorophenyl)-4-methyl pyrazolidin-3-one

(d)

1,2-bis(4-chlorophenyl)-4-(2-ethylbutyl) pyrazolidine-3,5-dione

(e)

1,2-bis(4-chlorophenyl)-4-(4-(trifluoromethoxy)benzoyl) pyrazolidine-3,5-dione

(f)

Current work
(R=alkyl substituent)

Fig 1. Some bioactive and previously reported pyrazolidine derivative.

https://doi.org/10.1371/journal.pone.0298232.g001

Materials and methods

Chemistry

From Sigma-Aldrich in St. Louis, Missouri, United States, all analytical-grade chemicals were acquired. Melting points were noted in the open capillary tubes. FTIR (4000–400 cm^{-1}) was checked from Thermo Scientific Nicolet iS5. NMR spectra (^{1}H and ^{13}C) were checked with Bruker (DRX-75 and 300 MHz) instrumentation. The elements C, H, S, and N were examined using a Vario EL III elemental analyzer. Mass spectrum was employed using PerkinElmer GCMS model Clarus sq8 (EI).

Synthesis of 4-(1-hydrazinyl-3-phenylallyl)pyrazolidine-3,5-dione (1a)

A mixture 1.32 mL of cinnamaldehyde (0.01 mol), 1.20 mL of pyrazolidine-3,5-dione (0.01 mol), hydrazine (0.01 mol) and 0.5 g of Cu(II)-tyr enzyme were mixed in a grout and powdered at ambient temperature. To recover the catalyst, pH 6.0 potassium phosphate buffer (2 mL, 50 mM) was added and the mixture was filtered. The progress of the reaction was monitored by TLC. Column chromatography (Ethyl acetate 4: hexane 6) was used to separate the final solid material, the procedure was followed by remaining compounds **1(b-m)**. Detailed physical values, spectral, mass, and Analytical values of compounds (**1a-m**) were reported in supporting information (SI) file.

Biological activities

Larvicidal activity. The synthesis of (**1a-m**) was carried out according to a previously reported protocol [30] (More information in SI file).

Antifeedant activity. The compounds were examined for antifeedant activity and assessed in aquatic species that were not intended targets. The antifeedant activity was assessed using a previously described method [30] (More information in SI file).

Molecular docking study

Molecular docking experiments were conducted to evaluate the binding and interaction of compound **1c**, permethrin, and 3OGN protein using AutoDock Vina 1.1.2 software (http://mgltools.scripps.edu) [31]. The detailed experimental given in SI file.

MD simulation

To assess the stability of the docked complexes found by IFD analysis, a molecular dynamics simulation was performed using Desmond (Schrodinger Biosuite). The MD simulation procedure followed a previously reported method [32, 33].

DFT calculation

Comparable theoretical data were obtained by DFT calculations using the B3LYP/6–31G (d, p) basis set. These results were congruent with the experimental findings from FT-IR, and the energy gap between the HOMO and LUMO [34]. The detailed experimental given in SI section.

Results and discussion

Chemistry

In a one-pot multicomponent synthesis, a series of pyrazolidine-3,5-dione derivatives (**1a-m**) were prepared using Cu(II)tyrosinase as the catalyst and the grindstone technique. A mixture
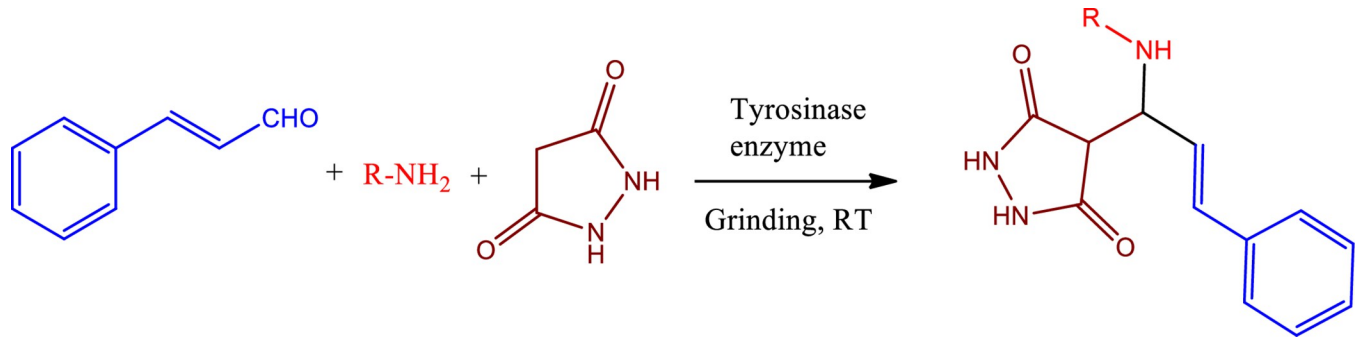
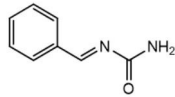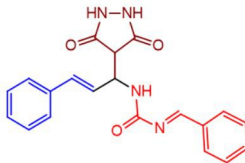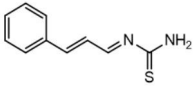**Scheme 1. Synthetic pathway for the Mannich base derivative.**
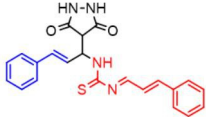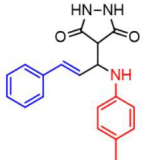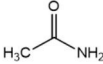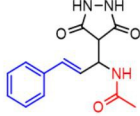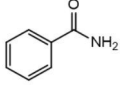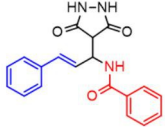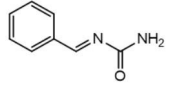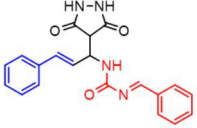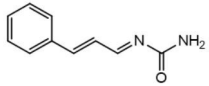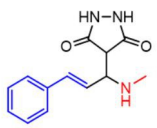
of pyrazolidine-3,5-dione, cinnamaldehyde, hydrazine hydrate, and catalytic amounts of the Cu(II)-Tyr enzyme was ground in a mortar and subsequently purified by column chromatography. Scheme 1 depicts the general layout of the synthetic pathway for the Mannich base derivative. The amines and chemicals used to optimize the reaction conditions are detailed in Table 1.

Table 1. Optimization of reactants and yield with final product for compounds (1a-m).

Compounds	-R	Final product	Yield (%)
1a	NH_2-NH_2		96
1b			91
1c			83
1d			87
1e			91

(Continued)

Table 1. (Continued)

Compounds	-R	Final product	Yield (%)
1f			92
1g			88
1h			84
1i			86
1j			83
1k			92
1l			94
1m	$H_3C\text{-}NH_2$		84

Various Cu(II) catalysts were employed to optimize the reaction using both the grindstone method without solvent and the conventional method with $CHCl_3$ solvent. The reaction for compound **1a** was conducted at room temperature, and a total of 14 catalysts were employed for its optimization. Cu(II)-catalysed reactions (0.5 equivalent) in the grindstone method at 2 min yielded lower compared to the conventional method. Conversely, no yield was obtained without a catalyst. Three enzyme catalysts were optimized for the reaction, with the tyrosinase from mushroom catalysing well compared to other enzyme catalysts. The tyrosinase-catalysed reaction achieved a 96% yield in the grindstone method without solvent, while the

conventional method yielded only 45% after 1 h of reaction time. The catalyst optimization results are summarized in Table 2.

However, the Cu(II)acetylacetonate catalyst in various solvents (toluene, CHCl$_3$, n-hexane, CH$_2$Cl$_2$, THF, and dichloroethane) at room temperature yielded product **1a** in varying percentages, namely 32%, 36%, 22%, 13%, 15%, and 10%, respectively. When the reaction was conducted in CHCl$_3$ under reflux, a significantly higher yield of 57% was achieved (Table 3, entry 6). Conversely, the presence of catalysts, including CuCl$_2$, at room temperature for a maximum of 2 minutes resulted in a lower yield of 12% (Table 2, entry 2). The Cu(II) tyrosinase catalyst (0.5 equivalent) at room temperature provided a high yield of 92%, and using 1 equivalent of this catalyst yielded an even higher percentage of 96% (entry 14, Table 2), surpassing yields obtained with much higher proportions of other catalysts (0.5 equiv.).

In Scheme 2, we propose a model of the Cu(II)-Tyr-catalysed Mannich reaction. The Schiff base is initially formed by the reaction of an aldehyde and an amine, and pyrazolidine-3,5-dione is preactivated by Cu(II)-Tyr, yielding the enolate anion. Subsequently, the Schiff base collaborates with the Cu(II)-Tyr-His molecule to create an intermediate complex.

Mannich base reactions relying on Cu-containing substances, such as Cu(CF$_3$SO$_4$)$_2$, Cu(CH$_3$COO)$_2$, CuBr, and Cu NPs, as well as enzymes like trypsin, lipase, and protease, have been employed to catalyse the one-pot multicomponent Mannich process. This study focused on the synthesis of *N*-Mannich base derivatives (**1a-m**), which were catalysed by a copper-containing enzyme called Cu(II)-Tyr.

The catalysts were optimized using trypsin, lipase, CuCl$_2$.2H$_2$O, and Cu(II)-Tyr, resulting in yields of 55%, 61%, 12%, and 92%, respectively. Table 2 outlines the optimized reaction conditions for the catalysts, which were employed to assess the reaction yield. No reaction occurred without solvent, even after 2 h of reflux at room temperature using the conventional method. Acetonitrile as the solvent under reflux produced a 19% yield after 2 h, while methanol and ethanol yielded 35% and 31% at 2 h, respectively (Table 3, entries 2,3). In contrast, using benzene as the medium enhanced the yield to 21% (Table 3, entry 4). However, all solvents tested were less active than CHCl$_3$, which exhibited high activity after 2 h. The optimization of the solvent and its performance is summarized in Table 3.

Table 2. Catalyst optimization for compound 1a with room temperature.

Entry	Catalyst	Equiv.	Grindstone method Without solvent		Conversional method With CHCl$_3$	
			Time (min)	Yield (%)	Time (min)	Yield (%)
1	No catalysis		2	-	30	-
2	CuCl$_2$.2H$_2$O	0.5	2	12	30	22
3	Copper(II) oxide	0.5	2	14	30	25
4	CuSO$_4$	0.5	2	15	30	22
5	Cu(OTf)$_2$	0.5	2	10	30	23
6	Dichloro(1,10-phenanthroline) copper(II)	0.5	2	-	30	-
7	Copper(II) *tert*-butylacetoacetate	0.5	2	-	30	-
8	Copper(II) acetate	0.5	2	6	3	12
9	Copper(II) acetylacetonate	0.5	2	-	30	10
10	Ammonium tetrachlorocuprate(II) dehydrate (NH$_4$)$_2$CuCl$_4$ · 2H$_2$O	0.5	2	-	30	-
11	copper(II)ethyl acetoacetate	0.5	2	5	30	18
12	Trypsin from bovine pancreas	0.5	2	55	30	22
13	Lipase from Candida antarctica	0.5	2	61	30	26
14	Cu(II)-Tyrosinase from mushroom	**0.5**	**2**	**92**	**30**	**36**
		1	5	96	1hr	45

Table 3. Optimization of solvent using conversion method synthesis of compound 1a.

Entry	Solvent	Condition Reflux, rt	Yield [%]
1	No solvent	30min	-
		1hr	-
		2hr	32
1	Acetonitrile	30min	10
		1hr	16
		2hr	19
2	Methanol	30min	20
		1hr	23
		2hr	35
3	Ethanol	30min	17
		1hr	23
		2hr	31
4	Benzene	30min	9
		1hr	15
		2hr	21
5	Toluene	30min	32
		1hr	40
		2hr	48
6	**CHCl$_3$**	**30min**	**36**
		1hr	**45**
		2hr	**57**
7	n-hexane	30min	22
		1hr	36
		2hr	40
8	CH$_2$Cl$_2$	30min	13
		1hr	24
		2hr	32
9	THF	30min	15
		1hr	26
		2hr	36
10	Dichloroethane	30min	10
		1hr	15
		2hr	20

https://doi.org/10.1371/journal.pone.0298232.t003

NMR (^{1}H and ^{13}C) and FT-IR spectroscopies were employed to evaluate the synthesised compounds. In the IR spectra, the compounds exhibited significant bands indicative of– NH–,–CO, and–C = C–groups at 3495–3571, 1700–1767, and 1610–1680 cm^{-1}, respectively. The ^{1}H NMR signals were observed at 8.03–2.0, 7.40–7.24, and 6.56 ppm, corresponding to -NH, Ph-ring, and Ph-CH protons. The ^{13}C NMR displayed peaks at 207.1–164.5, 136.4– 127.9, and 56.2–45.4 ppm, corresponding to -CO, -Ph-ring, and -NH-CH- atoms, respectively. The conformation of each synthesised compound was confirmed through mass spectrometry and elemental analysis. Detailed Mass, FTIR, and NMR (^{1}H and ^{13}C) spectra are provided in the SI (S1-S52 Figs in S1 File).

"Imine precursors are often used to organise *E*-alkenyl imines from equivalent *E*-alkenyl aldehydes. The process involves the formation of carbon-carbon bonds, which enables the conversion of in situ generated *E*-alkenyl imine from E-alkenyl aldehydes and secondary
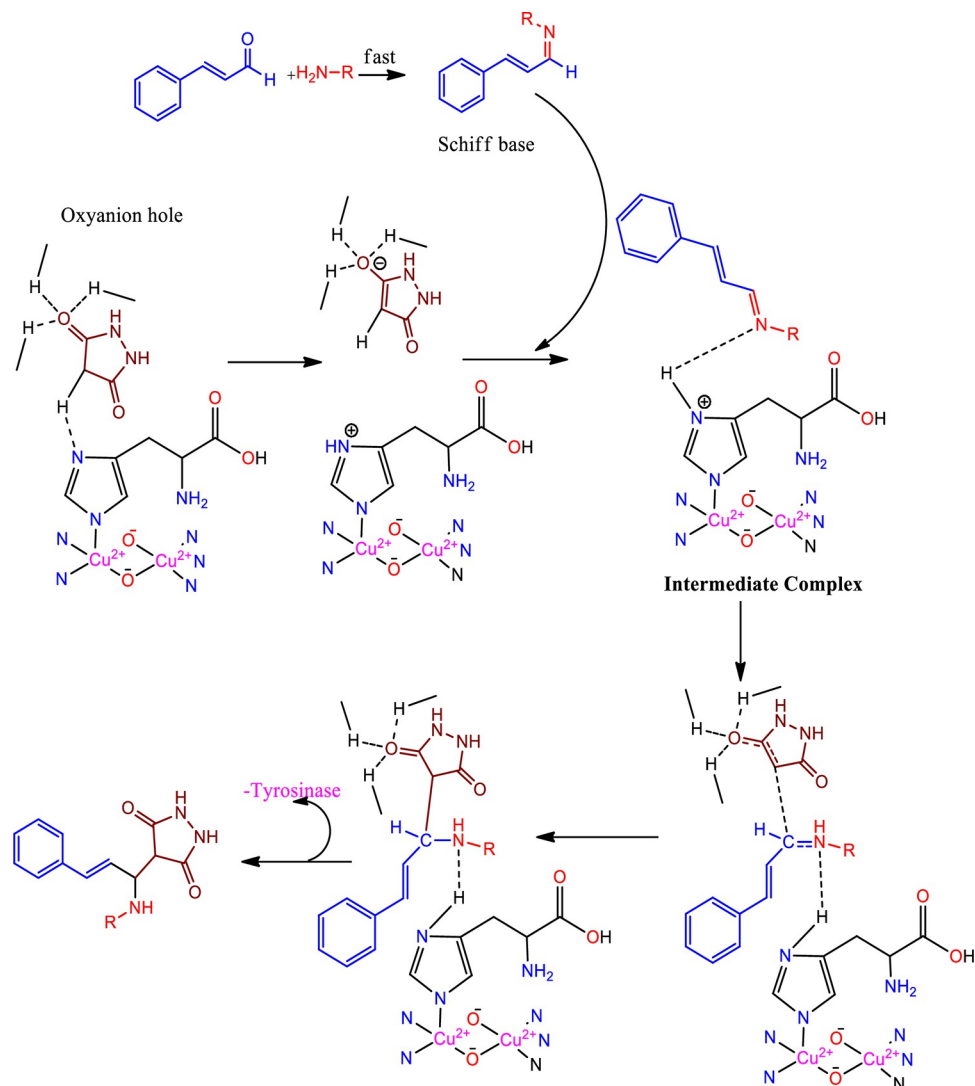
Scheme 2. Mechanism of the synthesis of compound 1a.

amines, as well as acetophenone, in the presence of 5 mol% Cu(II)-tyrosinase catalyst. This results in the production of Mannich adducts (**1a-m**) with moderate to good yields and high *E*-selectivity". The stereochemistry of the *E* isomers in compound **1a** was unequivocally established by NOE NMR data (see S1 File), which is supported by the following evidence. Consequently, the results of this study show that the downfield shift in the spectroscopic characteristics is more pronounced for the *E*-isomer of pyrazolidine-3,5-dione than for the *Z*-isomer [35].

Catalyst recovery studies

At least 10 recycling runs were performed to test the catalytic efficiency. The recyclability of the catalyst was analysed using compound **1a** in the Cu(II)-Tyr enzyme catalyst (Fig 2). The 1st use of the catalyst reached 92%, whereas the 2nd and up to 10th cycles of the reaction were readily used in low yields compared to the 1st cycle of the reaction.
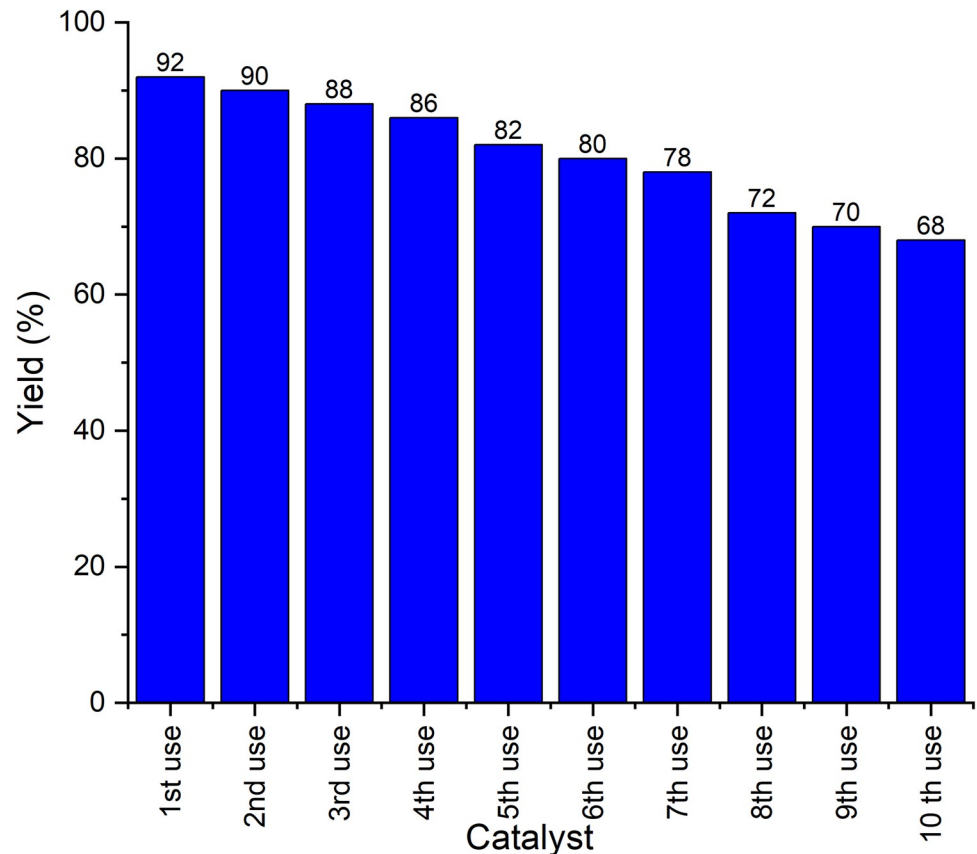
Fig 2. Recovery of catalyst.

Biological activity

Larvicidal activity. The effectiveness of the synthesised compounds **1(a-m)** was assessed in *C. quinquefasciatus* (second-instar larvae). Compound **1c** caused 100% mortality at 100 μg/mL, whereas compounds **1a**, **1f**, **1g**, and **1m** caused 80% mortality at the same concentration. Compound **1c** was highly active (LD_{50} value of 9.7 μg/mL) compared with permethrin (LD_{50} value of 17.1 μg/mL) and other compounds. Compounds **1a**, **1b**, and **1(d-m)** showed low activity against compound **1c** and permethrin. Because of their chemical performance, compounds **1f** and **1g** were equipotential active (LD_{50} values of 58.7 and 59.4 μg/mL); yet, the biological activity was manifested in distinct ways by a few significant functional groups. Table 4 shows that Larvicidal activity of compounds **1(a-m)**.

Antifeedant activity. The harmfulness of the synthesised compounds was investigated using antifeedant activity (marine fish *O. mossambicus*). Many of the synthesised compounds were highly toxic. Compounds **1a**, **1f**, **1g**, **1j**, and **1k** exhibited 100% mortality at 100 μg/mL, whereas compounds **1c** and **1d** were less toxic, with 0% mortality at 100 μg/mL. Compound **1e** was highly active (LD_{50} value of 9.7 μg/mL) compared with other compounds. Compounds **1j** and **1k** showed equipotential activity owing to the presence of different functional groups. Table 5 presents the antifeedant activity results.

Molecular docking

AutoDock Vina software was used to conduct molecular docking studies. The highly active compound **1c** was compared with permethrin concerning 3OGN protein. Compound **1c**

Table 4. Larvicidal activity of pyrazolidine-3,5-dione derivatives (1a-m).

Compounds	% of Mortality at concentration (µg/mL)			LD_{50} (µg/mL)[a]
	25	50	100	
1a	25.3 ± 0.4	46.9 ± 0.1	82.2 ± 0.6	56.4
1b	15.6 ± 0.7	29.3 ± 0.5	45.1 ± 0.2	>100
1c	53.8 ± 0.1	81.1 ± 0.1	100 ± 0.0	9.7
1d	21.3 ± 0.1	34.3 ± 0.2	45.4 ± 0.2	>100
1e	33.3 ± 0.1	48.3 ± 0.2	60.4 ± 0.2	66.1
1f	25.0 ± 0.2	44.1 ± 0.2	80.0 ± 0.2	58.7
1g	24.1 ± 0.2	43.2 ± 0.1	80.2 ± 0.2	59.4
1h	11.2 ± 0.2	27.1 ± 0.2	40.1 ± 0.1	>100
1i	19.3 ± 0.1	26.3 ± 0.1	40.2 ± 0.1	>100
1j	10.9 ± 0.1	21.7 ± 0.2	41.5 ± 0.1	>100
1k	31.0 ± 0.1	46.1 ± 0.1	59.4 ± 0.2	70.7
1l	24.1 ± 0.2	43.1 ± 0.2	78.1 ± 0.1	60.5
1m	29.0 ± 0.1	49.1 ± 0.1	83.0 ± 0.2	53.1
Permethrin	51.1 ± 1.0	76.3 ± 0.1	100 ± 0.0	17.1

[a] Values are presented as the mean ± SD (n = 3).

https://doi.org/10.1371/journal.pone.0298232.t004

exhibited a higher binding affinity (-10.4 kcal/mol) compared to standard permethrin (-9.5 kcal/mol). Table 6 presents the results for compound **1c** and standard permethrin with **3OGN**. Neither the standard nor the compound **1c** formed hydrogen bonds. In compound **1c**, residues TYR10, LEU15, LEU19, LEU58, PHE59, ALA62, VAL64, LEU73, LEU76, HIS77, LEU80, MET84, ALA88, MET89, MET91, GLY92, LEU96, HIS111, TRP114, HIS121, TYR122, and PHE123 engaged in hydrophobic connections. The interactions of compound **1c** helix (a), surface (b), 2D structure (c), and 3D structure are shown in Fig 3. (a) Hydrophobic, (b) ionizable, (c) aromatic, and (d) hydrogen bond surfaces at the interaction sites of **1c** and 3OGN are depicted in Fig 4. Amino acid residues LEU15, LEU19, LEU58, PHE59, ALA62, VAL64,

Table 5. Antifeedant activity of pyrazolidine-3,5-dione derivatives (1a-m).

Compounds	% of Mortality at concentration (µg/mL)				LD_{50} (µg/mL)[a]
	10	25	50	100	
1a	32.15 ± 0.21	68.19 ± 0.10	89.20 ± 0.15	100 ± 0.00	12.48
1b	20.12 ± 0.13	25.26 ± 0.30	31.08 ± 0.20	35.03 ± 0.83	>100
1c	0 ± 0.00	0 ± 0.00	0 ± 0.00	0 ± 0.00	>100
1d	0 ± 0.00	0 ± 0.00	0 ± 0.00	0 ± 0.00	>100
1e	41.02 ± 0.25	69.2 ± 0.14	83.98 ± 0.14	100 ± 0.00	6.01
1f	39.05 ± 0.74	50.13 ± 0.00	74.08 ± 0.00	100 ± 0.00	22.97
1g	-	06.21 ± 0.03	12.91 ± 0.23	23.55 ± 0.01	>100
1h	8.12 ± 0.02	15.13 ± 0.12	39.43 ± 0.10	43.09 ± 0.03	>100
1i	10.02 ± 0.12	20.26 ± 0.56	38.03 ± 0.01	46.09 ± 0.13	>100
1j	42.22 ± 0.41	59.25 ± 0.35	88.23 ± 0.00	100 ± 0.00	10.35
1k	33.12 ± 0.00	67.11 ± 0.74	87.87 ± 0.00	100 ± 0.00	12.84
1l	-	05.18 ± 0.13	10.31 ± 0.13	20.18 ± 0.13	>100
1m	0 ± 0.00	0 ± 0.00	0 ± 0.00	0 ± 0.00	>100

[a] Values are presented as the mean ± SD (n = 3).

https://doi.org/10.1371/journal.pone.0298232.t005

Table 6. Docking result of compound 1c and standard permethrin with 3OGN.

S. No	Compound/Drug	Dock Score	Interacting residues	Bond Length
1.	1c	-10.4	Phe 123	-
2.	Permethrin	-9.5	-	-

LEU73, LEU76, HIS77, LEU80, ALA88, MET89, MET91, GLY92, HIS111, TRP114, PHE123, and LEU124 are involved in hydrophobic interactions with each other in permethrin. The permethrin helix (a), surface (b), 2D structure (c), and 3D structural interactions are presented in Fig 5. (a) Hydrophobic, (b) ionizable, (c) aromatic, and (d) hydrogen bond surfaces at the interaction sites of permethrin and 3OGN are depicted in Fig 6 [36, 37].

(a) Helix

(b) surface

(c) 2D structure

(d) 3D structure
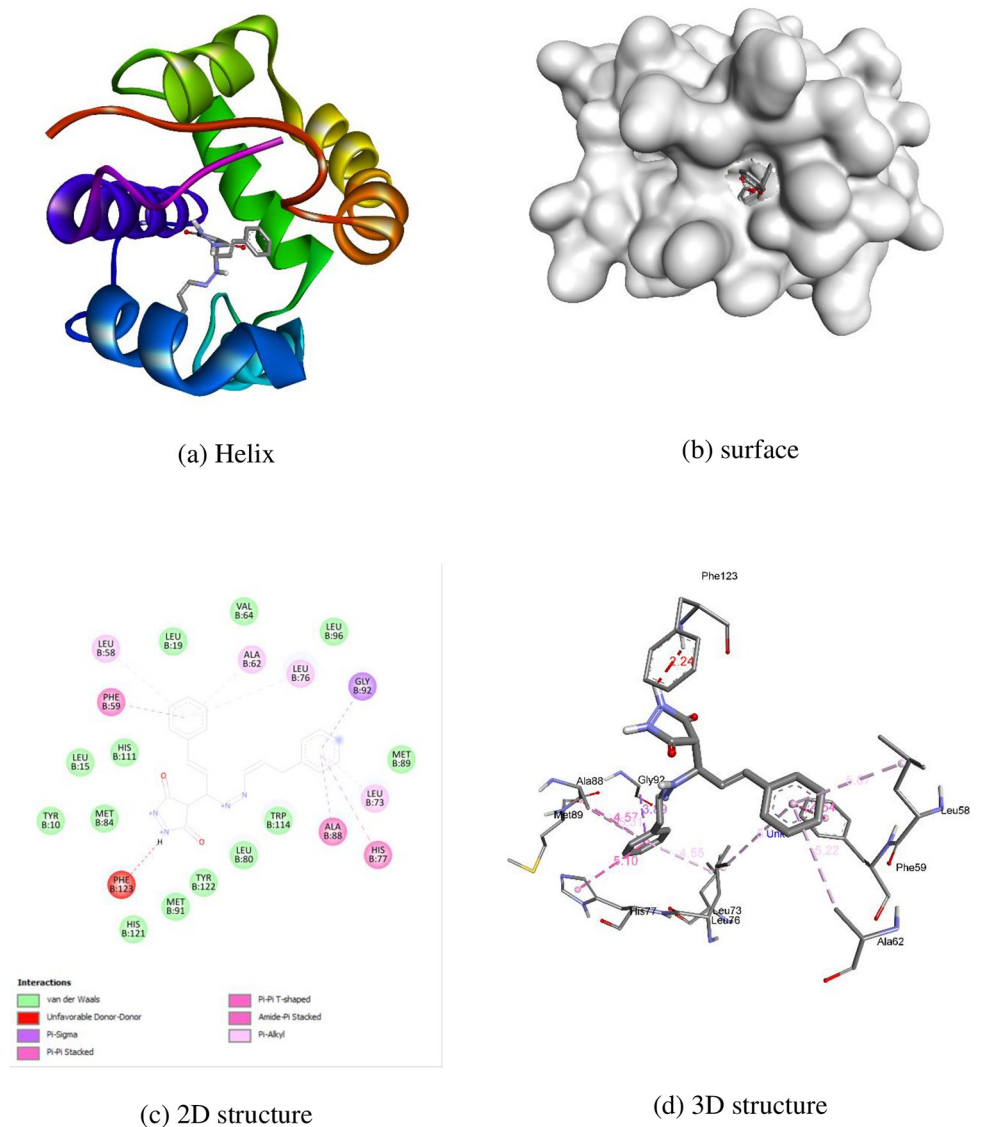
Fig 3. Molecular docking representation of compound 1c with 3OGN protein.
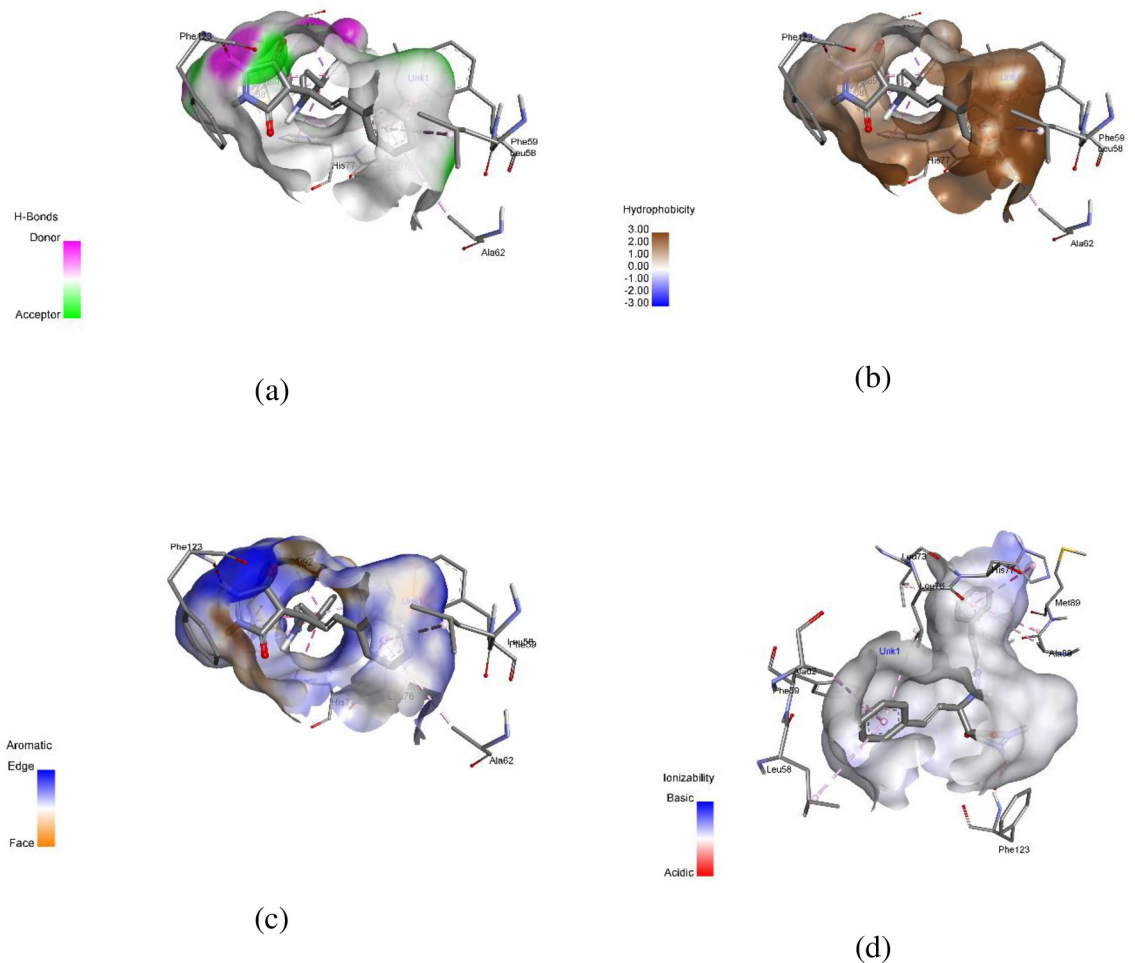
Fig 4. Representation of (a) hydrogen bonding, (b) hydrophobic interactions, (c) aromatic interactions, and (d) ionizability of the complex between 3OGN and compound **1c**.
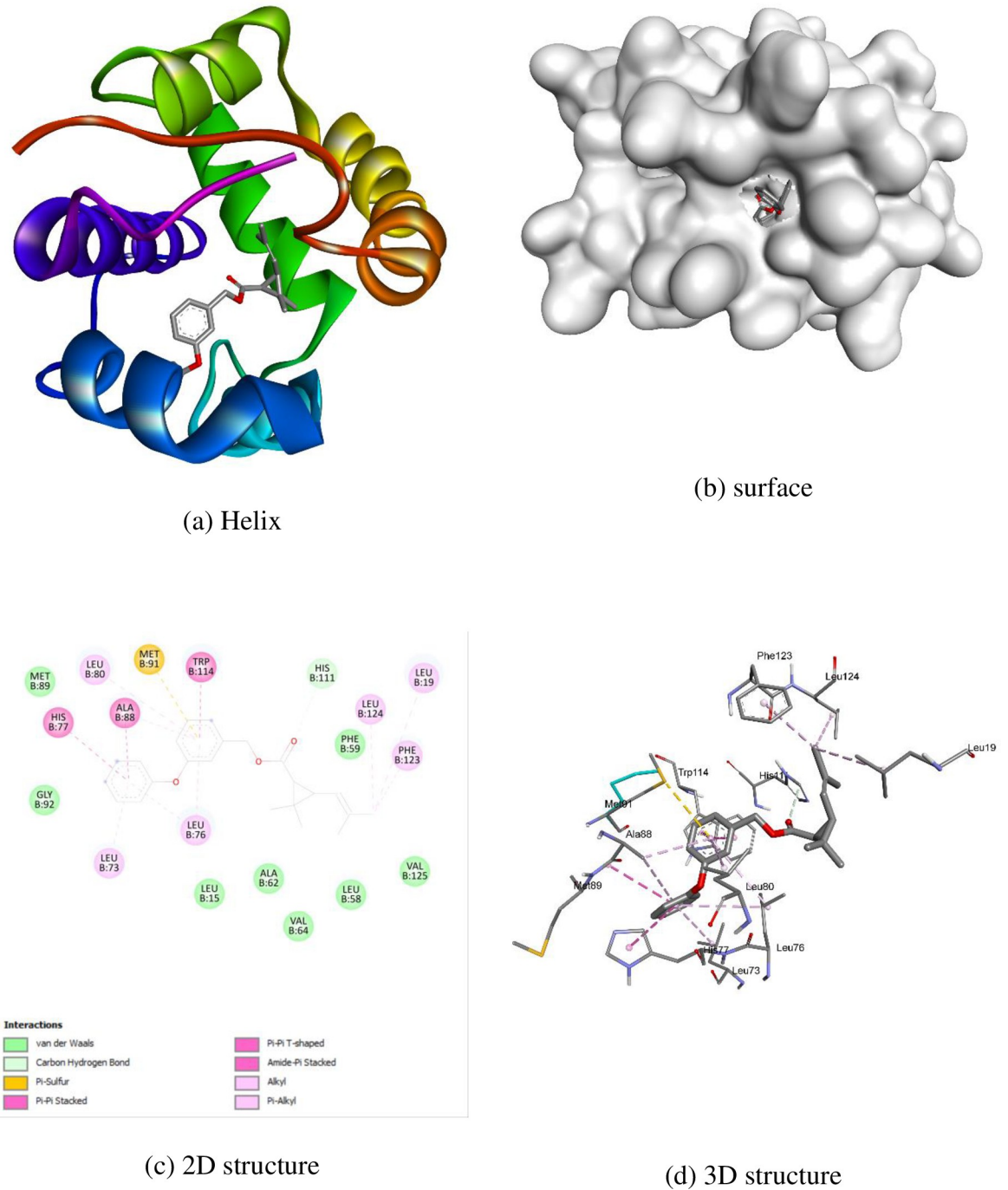
MD simulations

The stability of ligand 1c inside its docked complex with 3OGN was examined by molecular dynamics simulations using both Desmond and Schrödinger tools. The PRODRG server was employed to generate the ligand topology, which was subsequently combined with the protein topology using the GROMOS 43a1 force field and a solvation method utilising a single-point charge water model. The system was constructed with a cubic box that extended 2 nm from the protein surface. To ensure neutrality, the necessary ions were added, and the docked complex energy was minimised using the steepest descent algorithm.

The PME method was used to compute the electrostatics and bond lengths, which were subsequently constrained using the LINCS algorithm. The NVT and NPT ensembles were utilised to reach equilibrium in the systems for each 100 ps simulation, employing a V-rescale thermostat with a reference temperature of 300 K. For every 100 ps simulation, the NVT and NPT ensembles were used to bring the systems to equilibrium using a V-rescale thermostat set to 300 K as a reference. The coordinates of the docked complex structure were stored every 10 picoseconds (ps) for further study throughout the 10-nanosecond (ns) production MD

(a) Helix

(b) surface

(c) 2D structure

(d) 3D structure

Fig 5. Molecular docking representation of permethrin with 3OGN protein.

simulation, which used a 2-femtosecond (fs) time step. The analysis of the results was carried out using RMSD, RMSF, gyration, and hydrogen bond plots, and the graphs were plotted using Xmgrace software [38]. In previous studies, we compared molecular dynamics simulations to examine the interactions and stability of compounds with native ligands (permethrin) and their native ligands [39].

(a)

(b)

(c)

(d)
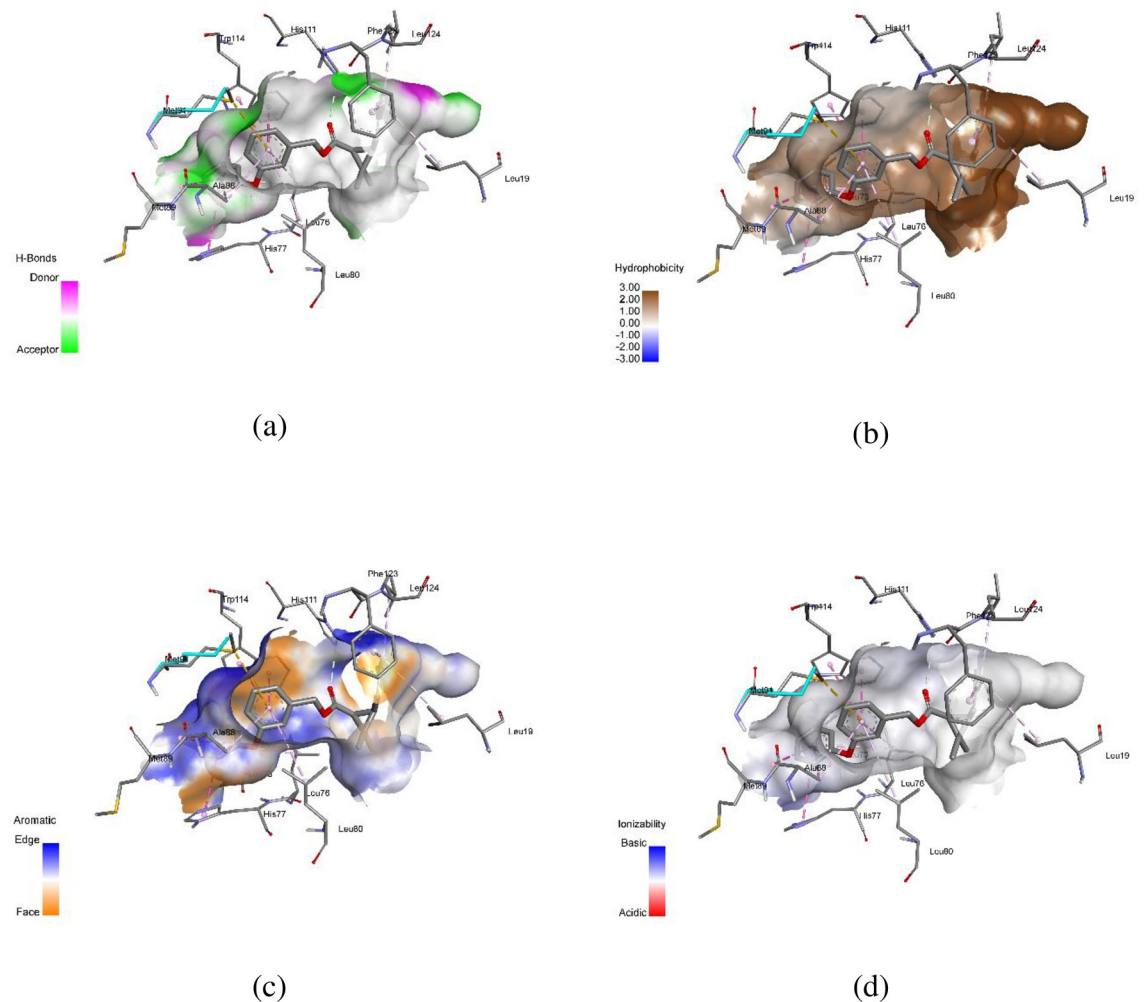
Fig 6. Representation of (a) hydrogen bonding, (b) hydrophobic interactions, (c) aromatic interactions, and (d) ionizability of the complex between 3OGN and permethrin.

https://doi.org/10.1371/journal.pone.0298232.g008

Root Mean Square Deviation (RMSD) analysis

The RMSD values are indicative of the stability of complex structures. The optimal position of compound **1c**, as determined by the highest docking score at 50 ns MD generated by Auto-Dock Vina, was selected for further analysis. After examining the RMSD plot of 3OGN with **1c**, it was determined that the complex remained stable between 30 and 40 ns, as well as between 20 and 40 ns. This was because the peak fluctuation of the Cα 3OGN protein and the heavy atoms of the ligand fell within the range depicted in Fig 7. RMSD analysis of 3OGN in the presence of **1c** revealed its stability.

Root Mean Square Fluctuation (RMSF) analysis

Alterations in the simulation's protein chain were assessed using RMSF analysis. No fluctuations were observed in the amino acid residues, except for the *N*- and *C*-terminal residues. All residues were within an unacceptable range (Fig 8A and 8B). Based on this MD simulation analysis, compound **1c** were stable and exhibited good interactions with important protein residues and timeline (Fig 9A and 9B). Therefore, these compounds may be effective inhibitors of the 3OGN proteins.

Fig 7. RMSD plot of 3OGN with 1c.

https://doi.org/10.1371/journal.pone.0298232.g009
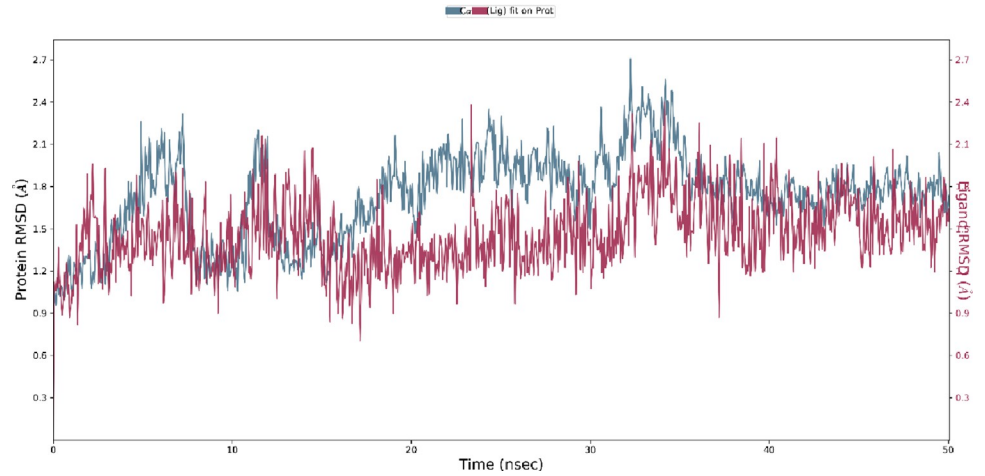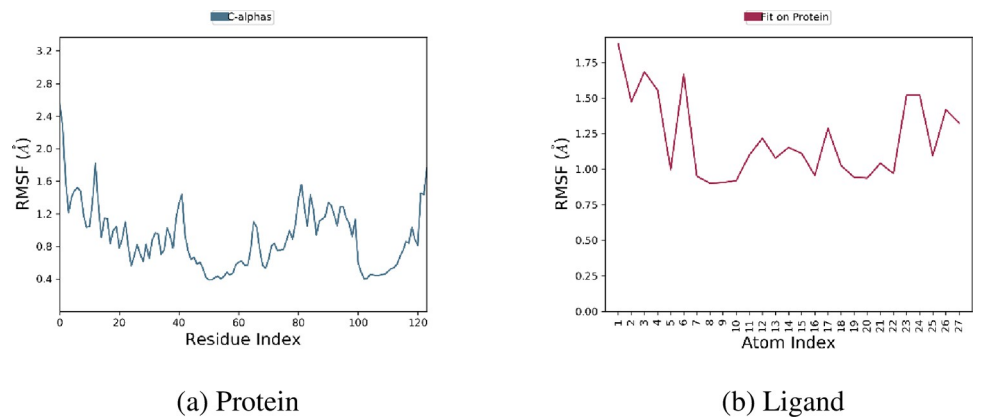
(a) Protein

(b) Ligand

Fig 8. RMSF plot of 3OGN with 1c.

https://doi.org/10.1371/journal.pone.0298232.g010
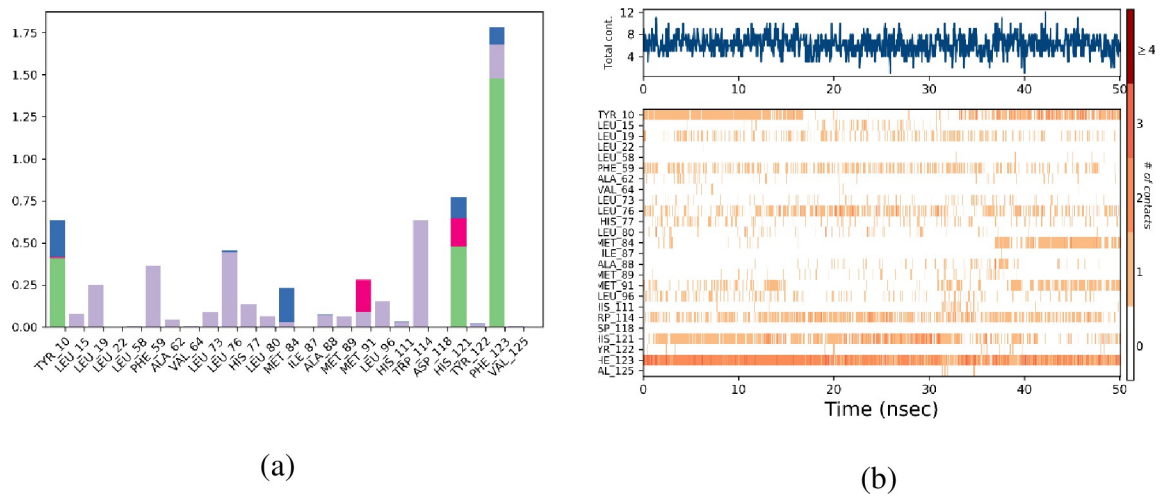
(a)

(b)

Fig 9. Histogram (a), and Timeline (b) representation of protein-ligand contacts of 3OGN with **1c**.

https://doi.org/10.1371/journal.pone.0298232.g011
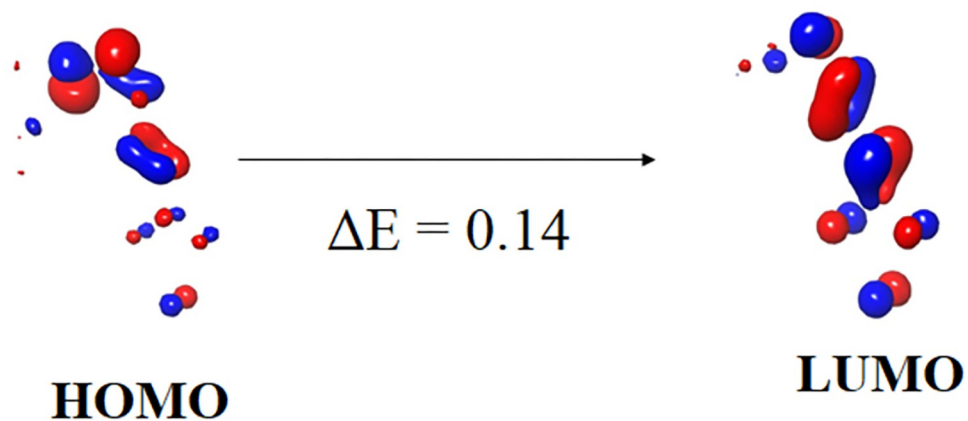
Fig 10. HOMO-LUMO energy diagram of compound 1c.

https://doi.org/10.1371/journal.pone.0298232.g012

(a)

(b)

(c)

(d)

Fig 11. Representation of (a) compound with atomic number, (b) Electron density, (c) Electrostatic potential, and (d) Interaction strength.

https://doi.org/10.1371/journal.pone.0298232.g013

(a) FT-IR

(b) VCD spectra

Fig 12. Shows the theoretical FT-IR (a) and VCD spectra (b) spectra of highly active compound 1c.

https://doi.org/10.1371/journal.pone.0298232.g014

DFT calculation

The B3LYP/6-31G (d, p) basis set was used to theoretically investigate the HOMO-LUMO, and FT-IR spectra [34, 40]. The highly active compound **1c** energy gap (ΔE) was 0.14 (Fig 10). Fig 11 shows th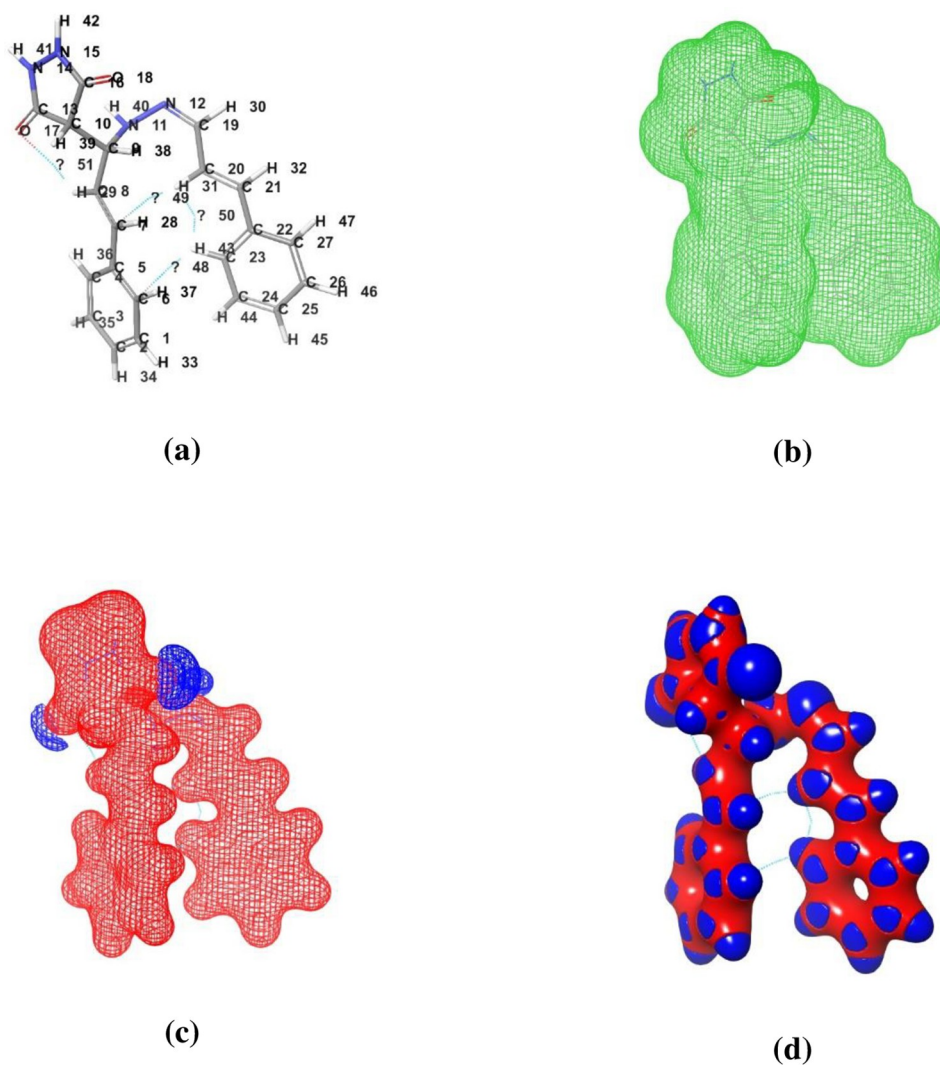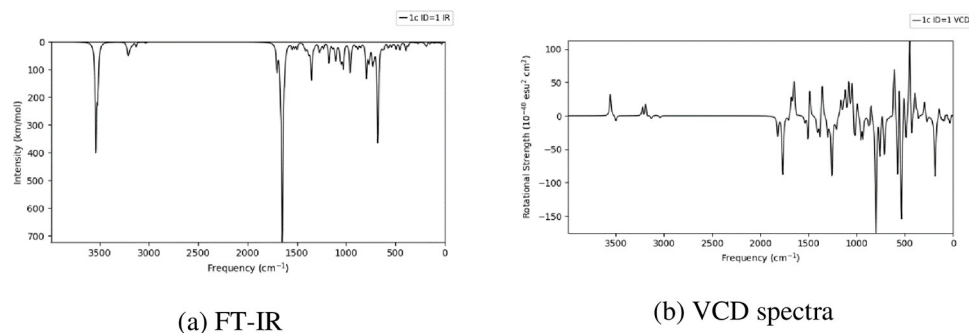e representation of (a) compound with atomic number, (b) electron density, (c) electrostatic potential, and (d) interaction strength of compound 1c. Fig 12 shows the theoretical FT-IR (a) and VCD spectra (b) spectra of highly active compound **1c**. A detailed discussion is provided in the supporting information file.

Conclusions

In this study, a novel one-pot multicomponent synthesis of pyrazolidine-3,5-dione derivatives (**1a-m**) was achieved via the grindstone method using Cu(II)-Tyr as a catalyst under mild reaction conditions, resulting in high yields (84–96%). The synthesised compounds (**1a-m**) were screened for larvicidal and antifeedant activities against *C. quinquefasciatus* and the marine fish *O. mossambicus*. In larvicidal activity, compound **1c** (LD_{50} value of 9.7 μg/mL) exhibited higher activity than standard permethrin (LD_{50} value of 17.1 μg/mL) and showed lower toxicity (0% mortality at 100 μg/mL) in antifeedant activity. The highly active compound **1c** was investigated by molecular docking using 3OGN, displaying higher binding affinity (-10.4 kcal/mol) than standard permethrin (-9.5 kcal/mol), and MD simulations were discussed. DFT calculations were performed on the highly active compound **1c**, and the HOMO-LUMO, and Fourier transform infrared (FTIR) values were calculated and discussed. This investigation concluded that the pyrazolidine-3,5-dione derivative of compound **1c** was the most effective insecticide, suggesting these compounds may serve as larvicidal agents and eco-friendly pesticides for pest control.

Supporting information

S1 File.
(PDF)

Acknowledgments

Author Contributions

Data curation: Omar H. Abd-Elkader.

Formal analysis: Anis Ahamed.

Methodology: Velmurugan Loganathan.

Software: Raman Gurusamy.

Supervision: Akbar Idhayadhulla.

Validation: SurendraKumar Radhakrishnan.

Writing – original draft: Akbar Idhayadhulla.

Writing – review & editing: Omar H. Abd-Elkader.

References

1. James AA. Mosquito molecular genetics: the hands that feed bite back. Science. 1992; 257: 37–38. https://doi.org/10.1126/science.1352413 PMID: 1352413

2. Yang YC, Lee SG, Lee HK, Kim MK, Lee SH. A piperidine amide extracted from Piper long um L. fruit shows activity against Aedesaegypti mosquito larvae. J. Agric. Food Chem. 2002; 50(50): 3765–3767. https://doi.org/10.1021/jf011708f PMID: 12059157

3. Cheng SS, Huang CG, Chen WJ, Kuo YH, Chang ST. Larvicidal activity of tectoquinone isolated from red heart wood type Cryptomeria japonica against two mosquito species. Bioresour Techno1. 2008; 99: 3617–3622. https://doi.org/10.1016/j.biortech.2007.07.038 PMID: 17804221

4. Álvarez L, Briceño A, Oviedo M. Resistance al Temephos en populations de Aedes aegypti (Diptera: Culicidae) of the west of Venezuela. Revista Colombiana de Entomología. 2006; 32(2): 172–175. https://doi.org/10.25100/socolen.v32i2.9386

5. Bisset J, Rodriguez M, Diaz C, Soca A. Estudio de la Resistencia en unacepa de Culex quinquefascia-tus, procedente de Medellı´n, Colombia. RevistaCubana de Medicina Tropical. 1998; 50: 133–137.

6. Isman MB. Botanical insecticides, deterrents, and repellents in modern agriculture and an increasingly regulated world. Annual Review of Entomology. 2006; 51: 45–66. https://doi.org/10.1146/annurev.ento.51.110104.151146 PMID: 16332203

7. Fajardo V, Podesta F, Urzu´a A. Resen˜a de los alcaloides encontrados en el ge´nero Berberis de Chile. Rev Lat Quím. 1986; 16: 141–156.

8. Leet J, Fajardo V, Freyer A, Shamma MM. Some dimericbenzylisoquinoline alkaloids with as unusual oxygenation pattern. J Nat Prod 1983; 46: 845–850. https://doi.org/10.1021/np50030a013

9. Baird A, Taylor C, Brayden D. Non-antibiotic anti-diarrhoeal drugs: Factors affecting oral bioavailability of berberine and loperamide in intestinal tissue. Adv Drug Deliv Rev. 1997; 23: 111–120. https://doi.org/10.1016/S0169-409X(96)00429-2

10. Barqi MM, Abdellah IM, Eletmany MR, Ali NM, Elhenawy AA, Abd El Latif FM, et al. Synthesis, Charac-terization, Bioactivity Screening and Computational Studies of Diphenyl– malonohydrazides and Pyri-dines Derivatives. ChemistrySelect. 2023; 8(2): e202203913. https://doi.org/10.1002/slct.202203913

11. Moydeen M, Kumar RS, Idhayadhulla A, Manilal A. Effective synthesis of some novel pyrazolidine-3, 5-dione derivatives via Mg (II) catalyzed in water medium and their anticancer and antimicrobial activities. Mol Divers. 2019; 23: 35–53. https://doi.org/10.1007/s11030-018-9850-3 PMID: 29974311

12. Abdellah IM, Eletmany MR, Abdelhamid AA, Alghamdi HS, Abdalla AN, Elhenawy AA, et al. One-pot synthesis of novel poly-substituted 3-cyanopyridines: Molecular docking, antimicrobial, cytotoxicity, and DFT/TD-DFT studies. J Mol Struct. 2023; 1289: 135864. https://doi.org/10.1016/j.molstruc.2023.135864

13. Koo KA, Kim ND, Chon YS, Jung MS, Lee BJ, Kim JH, et al. QSAR analysis of pyrazolidine-3,5-diones derivatives as Dyrk1A inhibitors. Bioorg Med Chem Lett. 2009; 19: 2324–2328. https://doi.org/10.1016/j.bmcl.2009.02.062 PMID: 19282176

14. Kapadia WJ, Azuine MA, Shigeta Y, Suzuki N, Tokuda H. Chemo preventive activities of etodolac and oxyphenbutazone against mouse skin carcinogenesis. Bioorg Med Chem Lett. 2020; 20: 2546–2548. https://doi.org/10.1016/j.bmcl.2010.02.093 PMID: 20299217

15. Denkert C, Kobel M, Berger S, Siegert A, Leclere A, Trefzer U, et al. Expression of cyclooxygenase 2 in human malignant melanoma. Cancer Res. 2001; 61: 303–308 PMID: 11196178

16. Uefuji K, Ichikura T, Mochizuki H. Cyclooxygenase-2 expression is related to prostaglandin biosynthesis and angiogenesis in human gastric cancer. Clin Cancer Res. 2000; 6: 135 138. PMID: 10656441

17. Shahroz MM, Sharma N. Experimental Investigation on Synthesis And Biological Evaluation Of Pyrazo-
     lidine-3,5-Dione. THI, 2019; 22(35): 139–146.

18. Mokbel SA, Fathalla RK, El-Sharkawy LY, Abadi AH, Engel M, Abdel-Halim M, et al. Synthesis of novel
     1,2-diarylpyrazolidin-3-one–based compounds and their evaluation as broad spectrum antibacterial
     agents. Bioorg Chem. 2020; 99: 103759. https://doi.org/10.1016/j.bioorg.2020.103759 PMID:
     32220665

19. Zhu YQ, Zou XM, Hu FZ. Synthesis and herbicidal evaluation of novel 3-[(a-hydroxy-substituted)benzy-
     lidene]pyrrolidine-2,4-diones. J Agric Food Chem. 2005; 53: 9566–9570. https://doi.org/10.1021/
     jf051510l PMID: 16302778

20. Sanchez-Ferrer A, Rodriguez-Lopez J, Garcia-Canovas F, Garcia-Carmona F. Tyrosinase: a compre-
     hensive review of its mechanism. Biochim Biophys Acta. 1995; 1247: 1–11. https://doi.org/10.1016/
     0167-4838(94)00204-t PMID: 7873577

21. Solomon EI, Sundaram UM, Machonkin TE. Multicopper oxidases and oxygenases. Chem Rev. 1996;
     96: 2563–2606. https://doi.org/10.1021/cr950046o PMID: 11848837

22. Solomon EI, Chen P, Metz M, Lee SK, Palmer A. Oxygen binding, activation, and reduction to water by
     copper proteins. Angew Chem Int Ed Engl. 2001; 40: 4570–4590. https://doi.org/10.1002/1521-3773
     (20011217)40:24<4570::aid-anie4570>3.0.co;2-4 PMID: 12404359

23. Rolff M, Schottenheim J, Decker H, Tuczek F. Copper-O_2 reactivity of tyrosinase models towards exter-
     nal monophenolic substrates: molecular mechanism and comparison with the enzyme. Chem Soc Rev.
     2011; 40: 4077–4098. https://doi.org/10.1039/C0CS00202J PMID: 21416076

24. Quist DA, Diaz DE, Liu JJ, Karlin KD. Activation of dioxygen by copper metalloproteins and insights
     from model complexes. J BioInorg Chem. 2017; 22: 253–288. https://doi.org/10.1007/s00775-016-
     1415-2 PMID: 27921179

25. Hamann JD, Herzigkeit B, Jurgeleit R, Tuczek F. Small-molecule models of tyrosinase: from ligand
     hydroxylation to catalytic monooxygenation of external substrates. Coord Chem Rev. 2017; 334: 54–
     66. https://doi.org/10.1016/j.ccr.2016.07.009

26. Ling-Ling W, Yang X, Da-Cheng Y, Zhi G, Yan-Hong H. Bio-catalytic asymmetric Mannich reaction of
     ketimines using wheat germ lipase. Catal. Sci. Technol. 2016; 6: 3963–3970. https://doi.org/10.1039/
     C5CY01923K

27. Mostafa AAF, SathishKumar C, Al-Askar AA, Sayed SR, SurendraKumar R, Idhayadhulla A, et al. Syn-
     thesis of novel benzopyran-connected pyrimidine and pyrazole derivatives via a green method using Cu
     (II)-tyrosinase enzyme catalyst as potential larvicidal, antifeedant activities. RSC Adv, 2019; 9(44);
     25533–25543. https://doi.org/10.1039/c9ra04496e PMID: 35530060

28. Chidambaram S, Mostafa AAF, Al-Askar AA, Sayed SR, Radhakrishnan S, Akbar I, et al. Green catalyst
     Cu(II)-enzyme-mediated eco-friendly synthesis of 2-pyrimidinamines as potential larvicides against
     Culex quinquefasciatus mosquito and toxicity investigation against non-target aquatic species. Bioorg
     Chem, 2021; 109, 104697. https://doi.org/10.1016/j.bioorg.2021.104697 PMID: 33652162

29. SathishKumar C, Keerthana S, Ahamed A, Arif IA, SurendraKumar R, Idhayadhulla A, et al. CuII-Tyrosi-
     nase Enzyme Catalyst-Mediated Synthesis of 2-Thioxopyrimidine Derivatives with Potential Mosquito
     Larvicidal Activity: Spectroscopic and Computational Investigation as well as Molecular Docking Inter-
     action with OBPs of Culex quinquefasciatus. ChemistrySelect, 2020; 5(15): 4567–4574. https://doi.org/
     10.1002/slct.202000060

30. Abdel-Fattah Mostafa A, Sathish Kumar C, Al-Askar AA, Sayed SRM, Surendra Kumar R, Idhayadhulla
     A, et al. Synthesis of novel benzopyran-connected pyrimidine and pyrazole derivatives via a green
     method using Cu(II)-tyrosinase enzyme catalyst as potential larvicidal, antifeedant activities. RSC Adv.
     2019; 9: 25533–25543. https://doi.org/10.1039/c9ra04496e PMID: 35530060

31. Trott O, Olson AJ. AutoDock Vina: improving the speed and accuracy of docking with a new scoring
     function, efficient optimization, and multithreading. J Comput Chem. 2010; 31: 455–461. https://doi.
     org/10.1002/jcc.21334 PMID: 19499576

32. Akram M, Lal H, Shakya S, Varshney R. Molecular engineering of complexation between RNA and bio-
     degradable cationic gemini surfactants: Role of the hydrophobic chain length. MSDE, 2022; 7(5), 487–
     506. https://doi.org/10.1039/D1ME00147G

33. Hussen NH, Hasan AH, Jamalis J, Shakya S, Chander S, Kharkwal H, et al. Potential inhibitory activity
     of phytoconstituents against black fungus: In silico ADMET, molecular docking and MD simulation stud-
     ies. Comput Toxicol. 2022; 24, 100247. https://doi.org/10.1016/j.comtox.2022.100247 PMID:
     36193218

34. Salih RHH, Hasan AH, Hussein AJ, Samad MK, Shakya S, Jamalis J, et al. One-pot synthesis, molecu-
     lar docking, ADMET, and DFT studies of novel pyrazolines as promising SARS-CoV-2 main protease
     inhibitors. Res Chem Intermed. 2022; 48(11), 4729–4751. https://doi.org/10.1007/s11164-022-04831-
     5

35. Chidambaram S, Ali D, Alarifi S, Gurusamy R, Radhakrishnan S, Akbar I, et al. Tyrosinase-mediated synthesis of larvicidal active 1, 5-diphenyl pent-4-en-1-one derivatives against Culex quinquefasciatus and investigation of their ichthyotoxicity. Sci Rep, 2021; 11(1), 20730. https://doi.org/10.1038/s41598-021-98281-5 PMID: 34671085

36. Alamri AS, Alhomrani M, Alsanie WF, Alyami H, Shakya S, Habeeballah H, et al. Enhancement of Haloperidol Binding Affinity to Dopamine Receptor via Forming a Charge-Transfer Complex with Picric Acid and 7,7,8,8-Tetracyanoquinodimethane for Improvement of the Antipsychotic Efficacy. Molecules, 2022; 27(10), 3295. https://doi.org/10.3390/molecules27103295 PMID: 35630772

37. Loganathan V, Ahamed A, Akbar I, Alarifi S, Raman G. Antioxidant, antibacterial, and cytotoxic activities of cimemoxin derivatives and their molecular docking studies. J King Saud Uni Sci. 2024; 36(1), 103011. https://doi.org/10.1016/j.jksus.2023.103011

38. Shakya S, Khan IM, Shakya B, Siddique YH, Varshney H, Jyoti S, et al., Protective effect of the newly synthesized and characterized charge transfer (CT) complex against arecoline induced toxicity in third-instar larvae of transgenic Drosophila melanogaster (hsp70-lacZ) Bg 9: experimental and theoretical mechanistic insights. J Mater Chem B. 2023; 11(6), 1262–1278. https://doi.org/10.1039/d2tb02362h PMID: 36648430

39. Feng D, Ren L, Wu J, Guo L, Han Z, Yang J, et al. Permethrin as a Potential Furin Inhibitor through a Novel Non-Competitive Allosteric Inhibition. Molecules. 2023; 28(4), 1883. https://doi.org/10.3390/molecules28041883 PMID: 36838867

40. Loganathan V, Akbar I, Ahamed A, Alodaini HA, Hatamelh AA, Abuthkir MS et al. Synthesis, Antimicrobial and Cytotoxic activities of Tetrazole N-Mannich Base Derivatives: Investigation of DFT calculation, Molecular Docking, and Swiss ADME Studies. Journal of Mol Struct, 2023; 137239. https://doi.org/10.1016/j.molstruc.2023.137239